

## The Thirring Model in $2+1d$ with Optimised Domain Wall Fermions

---

Simon Hands<sup>a,\*</sup> and Jude Worthy<sup>b</sup>

<sup>a</sup>*Department of Mathematical Sciences, University of Liverpool,  
Liverpool L69 3BX, United Kingdom*

<sup>b</sup>*Department of Physics, Swansea University,  
Singleton Park, Swansea SA2 8PP, United Kingdom*

*E-mail: [Simon.Hands@liverpool.ac.uk](mailto:Simon.Hands@liverpool.ac.uk), [judeworthy@gmail.com](mailto:judeworthy@gmail.com)*

After briefly reviewing the potential for the  $N$ -flavor Thirring model, formulated with reducible fermions in  $2+1d$ , to exhibit a strongly-coupled UV-stable fixed point where  $U(2N)$  symmetry is spontaneously broken by a fermion bilinear condensate, we present recent lattice studies using the Domain Wall Fermion formulation. In particular, we focus on possible improved methods for extracting the necessary  $L_s \rightarrow \infty$  limit, where  $L_s$  is the wall separation, through a combination of partial quenching (ie.  $L_s(\text{valence}) > L_s(\text{sea})$ ), replacing the Shamir kernel with the Wilson kernel in the definition of the overlap operator, and improved estimation of the signum function using the Zolotarev approximation. Equation of state fits for critical exponents on  $12^3$  systems yield encouraging agreement between distinct approaches, consistent with universal scaling, while contradicting earlier fits based on a naive extrapolation. The new results are also in tension with old results obtained with staggered fermions.

*The 40th International Symposium on Lattice Field Theory (Lattice 2023)  
July 31st - August 4th, 2023  
Fermi National Accelerator Laboratory*

---

\*Speaker

## 1. Introduction

The Thirring model is a covariant quantum field theory of interacting fermions with Lagrangian density

$$\mathcal{L} = \bar{\psi}_i(\not{\partial} + m)\psi_i + \frac{g^2}{2N}(\bar{\psi}_i\gamma_\mu\psi_i)^2. \quad (1)$$

Here the index  $i$  runs over  $N$  flavors. The contact interaction between currents is repulsive between like charges and attractive between opposite. In 2+1d we may specify the fields  $\psi, \bar{\psi}$  to lie in reducible representations of the spinor algebra, so that the Dirac matrices  $\gamma_\mu$  are  $4 \times 4$ , and there is a matrix  $\gamma_5 = \gamma_0\gamma_1\gamma_2\gamma_3$  such that  $\{\gamma_5, \gamma_\mu\} = 0$ . For sufficiently large interaction strength  $g^2$  and sufficiently small  $N$  the Fock vacuum may be disrupted through formation of a particle – antiparticle bilinear condensate

$$\langle \bar{\psi}\psi \rangle \equiv \frac{\partial \ln Z}{\partial m} \neq 0. \quad (2)$$

This results in a dynamically-generated mass gap at Dirac points where  $E(\vec{p}) = 0$ , in close analogy to chiral symmetry breaking in QCD. It has been hypothesised [1] that the transition to non-vanishing condensate at  $g_c^2(N)$  defines a Quantum Critical Point whose universal properties could perhaps characterise low energy electronic excitations in a planar material such as graphene. Such a fixed point would correspond to a strongly-interacting quantum field theory with *a priori* no small dimensionless parameters.

In the absence of a bare fermion mass the Lagrangian (1) is invariant under a global  $U(2N)$  generated by the following rotations:

$$\psi \mapsto e^{i\alpha}\psi \quad \bar{\psi} \mapsto \bar{\psi}e^{-i\alpha}; \quad \psi \mapsto e^{i\alpha\gamma_3}\psi, \quad \bar{\psi} \mapsto \bar{\psi}e^{-i\alpha\gamma_3}; \quad (3)$$

$$\psi \mapsto e^{i\alpha\gamma_5}\psi, \quad \bar{\psi} \mapsto \bar{\psi}e^{i\alpha\gamma_5}; \quad \psi \mapsto e^{i\alpha\gamma_3\gamma_5}\psi, \quad \bar{\psi} \mapsto \bar{\psi}e^{-i\alpha\gamma_3\gamma_5}. \quad (4)$$

Once  $m \neq 0$  (4) are no longer symmetries, so bilinear condensation results in a symmetry breaking  $U(2N) \rightarrow U(N) \otimes U(N)$ ; this should be compared to the pattern  $U(N) \otimes U(N) \rightarrow U(N)$  which pertains either to models built using staggered lattice fermions or continuum models using the Kähler-Dirac formulation of relativistic fermions [2].

## 2. Domain Wall Fermions

In a series of papers [3–5] we have studied the strong dynamics of this proposed symmetry breaking through lattice simulations with reducible fermions implemented through a domain wall construction of the form  $\mathcal{L}_{\text{kin}} = \bar{\Psi}(x, s)D_{DWF}\Psi(y, s')$ , where  $s, s'$  are coordinates along a fictitious third spatial direction, with open boundaries (ie. domain walls) separated by distance  $L_s$ . As  $L_s \rightarrow \infty$ , near zero-modes of  $D_{DWF}$  are localised on the walls as  $\pm$  eigenmodes of  $\gamma_3$ , and  $U(2N)$ -symmetric 2+1d physics described in terms of

$$\psi(x) = \mathcal{P}_-\Psi(x, 1) + \mathcal{P}_+\Psi(x, L_s); \quad \bar{\psi}(x) = \bar{\Psi}(x, L_s)\mathcal{P}_- + \bar{\Psi}(x, 1)\mathcal{P}_+, \quad (5)$$

with projectors  $\mathcal{P}_\pm = \frac{1}{2}(1 \pm \gamma_3)$ .

Now, for an arbitrary Dirac kernel  $D$  operating in the target  $2+1d$  space, the closest we can get to  $U(2N)$  symmetry is articulated by the Ginsparg-Wilson (GW) relations

$$\{\gamma_3, D\} = 2D\gamma_3D; \quad \{\gamma_5, D\} = 2D\gamma_5D; \quad [\gamma_3\gamma_5, D] = 0. \quad (6)$$

By construction (6) are satisfied by the  $2+1d$  overlap operator

$$D_{\text{ov}} = \frac{1}{2} \left[ (1+m) + (1-m) \frac{\mathcal{A}}{\sqrt{\mathcal{A}^\dagger \mathcal{A}}} \right]; \quad (7)$$

for the choice of *Shamir kernel*

$$\mathcal{A} = [2 + D_W - M]^{-1} [D_W - M], \quad (8)$$

with  $D_W$  the  $2+1d$  Wilson fermion kernel and  $Ma = O(1)$  the domain wall height, the overlap operator  $D_{\text{ov}}$  can be shown to be equivalent to the  $L_s \rightarrow \infty$  limit of  $D_{DWF}$  used to date [6]:

$$\lim_{L_s \rightarrow \infty} \frac{\det D_{DWF}(m)}{\det D_{DWF}(m=1)} = \det D_{\text{ov}}(m). \quad (9)$$

The four-fermion interaction in the Thirring model may be reproduced by the introduction of a

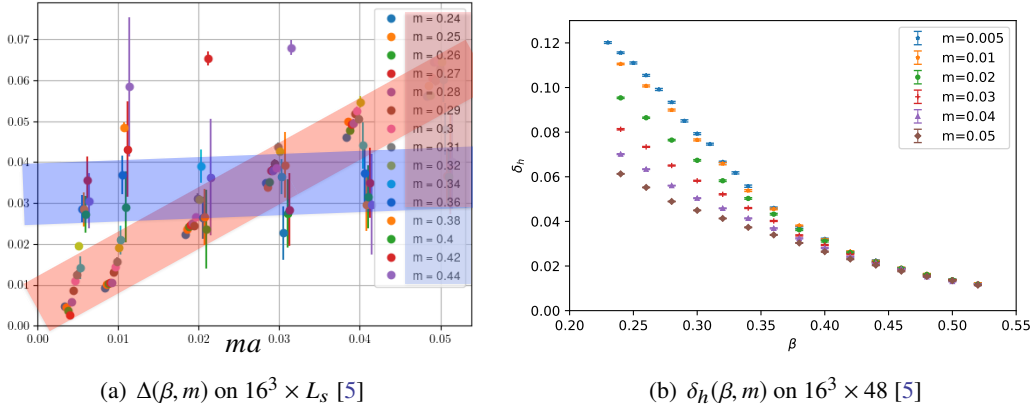


**Figure 1:** Quantifying the approach to  $L_s \rightarrow \infty$

bosonic vector auxiliary field  $A_\mu$  coupled to the conserved current  $i\bar{\psi}\gamma_\mu\psi$ . In the lattice model set out in [3–5],  $A_\mu$  is located on a link of the  $2+1d$  lattice and linearly coupled to the conserved DWF current which is defined throughout the bulk. Hence off-diagonal elements of  $D_{DWF}$  are of the form  $D_\mu \sim (1 + iA_\mu)$  rather than the canonical  $D_\mu \sim e^{iA_\mu}$  of abelian gauge theories: the link fields are thus non-compact and non-unitary, which makes inversion of  $D_{DWF}$  numerically challenging. We simulate the Thirring model with  $N = 1$  using the RHMC algorithm to reproduce the functional measure  $\sqrt{\det D_{DWF}^\dagger D_{DWF}}$  [4]. Taking  $L_s \rightarrow \infty$  is hard; we have fitted data from  $16^3 \times L_s = 8, 16, \dots, 80$  using an exponential *Ansatz*

$$\langle \bar{\psi}\psi \rangle_\infty - \langle \bar{\psi}\psi \rangle_{L_s} = A(\beta, m) e^{-\Delta(\beta, m)L_s}, \quad (10)$$

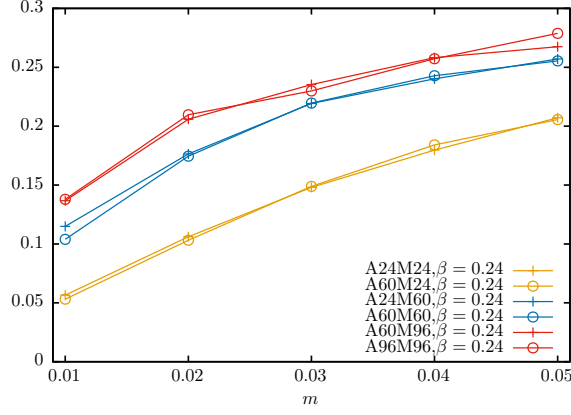


**Figure 2:** Bilinear condensate for Shamir kernel on  $12^3 \times L_s$  at  $\beta = 0.24$ , for various different  $L_s$ (sea) (labelled A in key), for  $L_s$ (valence) = 24 (yellow), 60 (blue), 96 (orange) (labelled M in key).

with inverse coupling  $\beta \equiv ag^{-2}$ . Fig. 1(a) shows a compendium of fitted values for  $\Delta$ . For weak coupling  $\beta > 0.4$ ,  $\Delta$  is roughly  $m$ -independent (blue band), but for stronger couplings  $\beta < 0.35$ ,  $\Delta \propto m$  (red band), implying that here the large- $L_s$  limit is extremely challenging in the massless limit. Fig. 1(b) shows a compendium of the residual  $\delta_h$  defined by

$$\delta_h \equiv \Im \langle \bar{\Psi}(1) \gamma_3 \Psi(L_s) \rangle \approx \frac{1}{2} (\langle \bar{\psi} \psi \rangle - i \langle \bar{\psi} \gamma_3 \psi \rangle) \quad (11)$$

which should vanish if the  $U(2N)$  symmetry relating the two condensates on the RHS is restored. Again, at fixed  $L_s$  and strong coupling the symmetry restoration becomes harder as  $m \rightarrow 0$ . Further results for the locality of  $D_{\text{ov}}$  and the restoration of the GW relations (6) can be found in [5].

### 3. Improving $L_s \rightarrow \infty$

Since lack of control of the  $L_s \rightarrow \infty$  limit casts doubt on the accuracy of earlier studies [4, 5], we have recently experimented with three strategies for ameliorating the problem. Further discussion can be found in [7].

- **Partial Quenching (PQ):** This is the most straightforward to implement. The main impact of finite  $L_s$  appears in measurements in the fermion sector (the chief example being the bilinear condensate order parameter itself), while the effect on the underlying bosonic  $A_\mu$  configurations is much milder, as exemplified in Fig. 2. Accordingly we have made studies with  $L_s(\text{sea}) \neq L_s(\text{valence})$ , the most straightforward choice being  $L_s(\text{sea}) \ll L_s(\text{valence})$ .
- **Wilson kernel:** We have replaced the Shamir kernel (8) in the definition (7) of  $D_{\text{ov}}$ , where the corresponding DWF operator is represented as an  $L_s \times L_s$  matrix<sup>1</sup>

$$D_{SHT} = \begin{pmatrix} D_W - M + I & -\mathcal{P}_- & 0 & im\mathcal{P}_+ \\ -\mathcal{P}_+ & D_W - M + I & -\mathcal{P}_- & 0 \\ 0 & -\mathcal{P}_+ & D_W - M + I & -\mathcal{P}_- \\ -im\mathcal{P}_- & 0 & -\mathcal{P}_+ & D_W - M + I \end{pmatrix} \quad (12)$$

<sup>1</sup>The corner elements in (12,13) are appropriate for a mass term  $im\bar{\psi}\gamma_3\psi$ , equivalent to  $m\bar{\psi}\psi$  after  $U(2N)$  rotation.

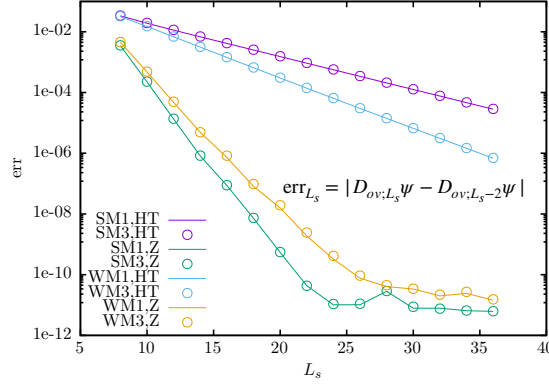


**Figure 3:** Convergence of the overlap with increasing  $L_s$  on a fixed  $12^3$  auxiliary background, for both Shamir and Wilson kernels, and mass terms  $m_1\bar{\psi}\psi$ ,  $m_3\bar{\psi}i\gamma_3\psi$ , with  $m_1a = m_3a = 0.05$ .

with the *Wilson kernel*  $\mathcal{A} = D_W - M$ , with DWF transcription

$$D_{WHT} = \begin{pmatrix} \mathcal{A} + I & (\mathcal{A} - I)\mathcal{P}_- & 0 & -im(\mathcal{A} - I)\mathcal{P}_+ \\ (\mathcal{A} - I)\mathcal{P}_+ & \mathcal{A} + I & (\mathcal{A} - I)\mathcal{P}_- & 0 \\ 0 & (\mathcal{A} - I)\mathcal{P}_+ & \mathcal{A} + I & (\mathcal{A} - I)\mathcal{P}_- \\ +im(\mathcal{A} - I)\mathcal{P}_- & 0 & (\mathcal{A} - I)\mathcal{P}_+ & \mathcal{A} + I \end{pmatrix} \quad (13)$$

which is much better-conditioned.

- **Improved Rational approximation for sgn:** The approach of  $D_{DWF}$  to  $D_{ov}$  at finite  $L_s$  depends on a rational approximation to  $\text{sgn}(\mathcal{A}) \equiv \mathcal{A}/\sqrt{\mathcal{A}^\dagger\mathcal{A}}$  expressed as a product of  $L_s$  factors. We have replaced the hyperbolic tangent (HT) form

$$\text{sgn}(x) \approx \tanh(L_s \tanh^{-1} x) = \frac{1 - \mathcal{T}_{HT}}{1 + \mathcal{T}_{HT}} \quad \text{with} \quad \mathcal{T}_{HT} = \left( \frac{1-x}{1+x} \right)^{L_s} \quad (14)$$

used in vanilla DWF [6] by the Zolotarev (Z) approximation

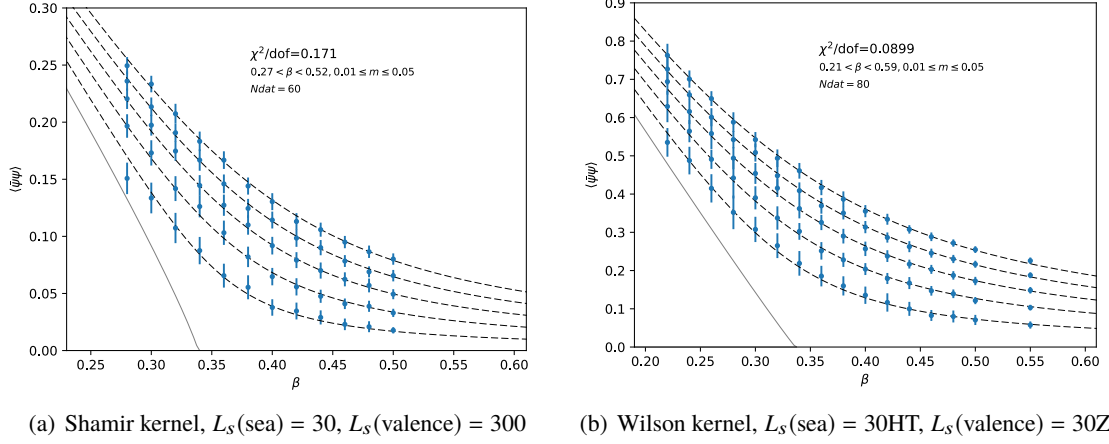
$$\text{sgn}(x) \approx \frac{1 - \mathcal{T}_Z}{1 + \mathcal{T}_Z} \equiv dx \frac{\prod_{m=1}^{L_s/2-1} (a_m - x^2)}{\prod_{m=1}^{L_s/2} (d_m - x^2)} \quad \text{with} \quad \mathcal{T}_Z = \prod_{s=1}^{L_s} \frac{1 - \omega_s x}{1 + \omega_s x}, \quad (15)$$

where the coefficients  $a_m, d_m, d$  depend on the applicable range of the approximation, chosen to match the spectral range of  $\mathcal{A}$  [8]. The superior  $L_s$ -convergence of Z over HT is shown in Fig. 3. The coefficients  $\omega_s$  found via the roots of  $\text{sgn}(x) = 1$  can be used to replace all instances of  $\mathcal{A}$  in the  $s$ th row of (13) by  $\omega_s\mathcal{A}$  to yield the *optimised* DWF introduced by Chiu [8].

#### 4. Results for the Equation of State

Since determination of the bilinear condensate on a finite system requires  $m \neq 0$ , our approach to characterising the critical properties is to fit a renormalisation group-inspired equation of state (EoS) to data collected in the critical regime but with  $m > 0$ :

$$m = A(g^{-2} - g_c^{-2})\langle\bar{\psi}\psi\rangle^{\delta-1/\beta} + B\langle\bar{\psi}\psi\rangle^\delta. \quad (16)$$

**Figure 4:** Thirring model equation of state on  $12^3$ 

	Shamir PQ $12^3$ $L_s(v) = 300\text{HT}$	Wilson PQ $12^3$ $L_s(v) = 30\text{Z}$	Shamir $16^3$ [5]	staggered $16^3$ [9]	staggered FSS [10]
$ag_c^{-2}$	0.339(24)	0.336(33)	0.283(1)	-	-
$\beta$	0.89(26)	1.04(29)	0.320(5)	0.57(2)	0.70(1)
$\delta$	2.07(40)	2.08(33)	4.17(5)	2.75(9)	2.63(2)
$\nu$	0.91(28)	1.1(3)	0.55(1)	0.71(3)	0.85(1)
$\eta$	0.96(18)	0.95(15)	0.16(1)	0.60(4)	0.65(1)

**Table 1:** Critical parameter fits

Data from a partially-quenched approach using the Shamir kernel is shown in Fig. 4(a) and from the Wilson kernel with Zolotarev approximation to  $\text{sgn}$  in the valence sector in Fig. 4(b). The fitted critical coupling  $ag_c^{-2}$  and exponents  $\beta, \delta$  are tabulated in Table 1, along with further exponents  $\nu, \eta$  estimated from hyperscaling. For comparison results from the earlier study [5] based on extrapolating Shamir kernel data to  $L_s \rightarrow \infty$  using the *Ansatz* (10), as well as two complementary studies of the Thirring model formulated with staggered lattice fermions, one using the HMC algorithm on fixed volume fitting the EoS (16) [9], and one using the fermion bag algorithm to perform a finite volume scaling analysis [10], are also shown.

Since Shamir and Wilson kernels are in effect two distinct regularisations of the Thirring model, we expect the derived critical exponents to coincide. While larger volumes and more statistics are needed to make definitive conclusions, the compatibility of the results from the two new approaches is encouraging, and consistent with universal scaling at a critical point for  $N = 1$ . The new results are also clearly incompatible with previous published results [5], suggesting that the exponential extrapolation (10) is not controlling the large- $L_s$  limit at accessible values of  $L_s$ ; in particular the approach seems to under-estimate the critical  $g_c^{-2}$ . Finally, it is worth remarking that the Thirring model defined using DWF yields distinct critical properties to those of the staggered fermion model, corroborating the claim that at a strongly-coupled continuum limit naive taste symmetry recovery cannot be assumed. Rather, it may well be that a distinct interacting fermion theory based on the

$U(N)\otimes U(N)$  symmetry of Kähler-Dirac fermions may exist, as outlined in [2].

## 5. Acknowledgements

This work used the DiRAC Data Intensive service (CSD3) at the University of Cambridge, managed by the University of Cambridge University Information Services on behalf of the STFC DiRAC HPC Facility ([www.dirac.ac.uk](http://www.dirac.ac.uk)). The DiRAC component of CSD3 at Cambridge was funded by BEIS, UKRI and STFC capital funding and STFC operations grants. DiRAC is part of the UKRI Digital Research Infrastructure. Further work was performed on the Sunbird facility of Supercomputing Wales. The work of JW was supported by an EPSRC studentship, and of SH by STFC Consolidated Grant ST/ST000813/1.

## References

- [1] D.T. Son, Phys. Rev. B **75** (2007) no.23, 235423 doi:10.1103/PhysRevB.75.235423.
- [2] S. Hands, Symmetry **13** (2021) no.8, 1523 doi:10.3390/sym13081523.
- [3] S. Hands, JHEP **11** (2016), 015 doi:10.1007/JHEP11(2016)015.
- [4] S. Hands, Phys. Rev. D **99** (2019) no.3, 034504 doi:10.1103/PhysRevD.99.034504.
- [5] S. Hands, M. Mesiti and J. Worthy, Phys. Rev. D **102** (2020) no.9, 094502 doi:10.1103/PhysRevD.102.094502.
- [6] S. Hands, Phys. Lett. B **754** (2016), 264-269 doi:10.1016/j.physletb.2016.01.037.
- [7] J. Worthy and S. Hands, PoS **LATTICE2021** (2022), 317 doi:10.22323/1.396.0317.
- [8] T.W. Chiu, Phys. Rev. Lett. **90** (2003), 071601 doi:10.1103/PhysRevLett.90.071601.
- [9] L. Del Debbio *et al.* [UKQCD], Nucl. Phys. B **502** (1997), 269-308 doi:10.1016/S0550-3213(97)00435-5.
- [10] S. Chandrasekharan and A. Li, Phys. Rev. Lett. **108** (2012), 140404 doi:10.1103/PhysRevLett.108.140404.